Published in final edited form as:
Nanomedicine. 2014 November ; 10(8): 1609–1617. doi:10.1016/j.nano.2014.05.006.

Gold Nanoparticle Hyperthermia Reduces Radiotherapy Dose

James F. Hainfeld, Ph.D.,
Nanoprobes, Inc., 95 Horseblock Rd., Unit 1, Yaphank, New York, 11980, USA; tel: 631-205-9490, fax: 631-205-9493

Lynn Lin, B.A.,
Nanoprobes, Inc

Daniel N. Slatkin, M.D.,
Nanoprobes, Inc

F. Avraham Dilmanian, Ph.D.,
Department of Radiation Oncology, State University of New York at Stony Brook

Timothy M. Vadas, Ph.D., and
Department of Civil and Environmental Engineering, University of Connecticut

Henry M. Smilowitz, Ph.D.
Department of Cell Biology, University of Connecticut Health Center

James F. Hainfeld: hainfeld@nanoprobes.com

Abstract

Gold nanoparticles can absorb near infrared light, resulting in heating and ablation of tumors. Gold nanoparticles have also been used for enhancing the dose of X-rays in tumors during radiotherapy. The combination of hyperthermia and radiotherapy is synergistic, importantly allowing a reduction in X-ray dose with improved therapeutic results. Here we intratumorally infused small 15 nm gold nanoparticles engineered to be transformed from infrared-transparent to infrared-absorptive by the tumor, which were then heated by infrared followed by X-ray treatment. Synergy was studied using a very radioresistant subcutaneous squamous cell carcinoma (SCCVII) in mice. It was found that the dose required to control 50% of the tumors, normally 55 Gy, could be reduced to <15 Gy (a factor of >3.7). Gold nanoparticles therefore provide a method to combine hyperthermia and radiotherapy to drastically reduce the X-ray radiation needed, thus sparing normal tissue, reducing the side effects, and making radiotherapy more effective.

Correspondence to: James F. Hainfeld, hainfeld@nanoprobes.com.

Conflict of interest statement: James F. Hainfeld is part owner of Nanoprobes, Inc. Other authors have no conflicting or financial interests.

Keywords

gold nanoparticles; hyperthermia; radiotherapy; cancer

Introduction

Radiotherapy continues to be a mainstay of cancer therapy due to its proven ability to kill cells and shrink tumors. Unfortunately, the dose typically has to be reduced below the curative level to spare vital surrounding tissue. Dividing cells are most radiosensitive, so large regions of the body including the abdomen and pelvis, where intestinal cells are rapidly dividing limit effective X-ray treatment. Unfortunately, many cancers are diagnosed after metastasis, and curative radiotherapy is prohibited due to the limiting dose normal tissues can tolerate. A method to increase dose specifically to tumor tissue would be beneficial.

Another way to kill cells is by overheating them, causing catastrophic death (necrosis) or heating to a milder temperature causing apoptosis. Heat also causes alterations of the tumor microenvironment, signal transduction, and reduction of drug resistance [1]. Hyperthermia (typically 40–45° C) induces heat shock proteins (e.g., HSP70) that confer a transient thermotolerance to subsequent higher, normally lethal temperatures [2]. Generally there is a lag of a few hours after which thermotolerance increases, peaking within 24 hours, then declining over a few hours to several days [3]. Heat also enhances ataxia telangiectasia mutated (ATM) kinase autophosphorylation activity impairing DNA double-strand break repair [2]. Hyperthermia alters blood flow: mild hyperthermia (<42–43° C) increases blood flow via vasodilation, but at higher temperatures blood flow decreases and vascular collapse can occur [3–6]. Heating to 42.5° C for 1 hour increased tumor, skin and muscle blood flow that peaked 16–48 hrs after heating [7]. Increased blood flow increases tumor oxygenation. However, mild hyperthermia alone (40–43°C for 60 min) is ineffective as a stand-alone therapy [8]. The rate at which cells are killed increases exponentially with temperature, doubling every degree from 39.5 to 50° C [9]. Higher temperatures cause catastrophic failures and rapid cell death. One reason is irreversible protein damage: albumin denatures at 45–62° C and IgGs at ~57° C [10, 11].

Clinical hyperthermia is usually implemented by microwave, radiofrequency, laser, or ultrasound. For example, in percutaneous microwave coagulation therapy (PMCT), a wire antenna is placed on the tip of a catheter guided arterially to liver or breast tumor masses. Application of 900–2450 MHz microwaves serves to heat tumors to ~65 °C [12], although the needle temperature may reach 119–160° C [13]. Phased multiple antenna arrays have been used to focus 433 MHz radiofrequency waves for head and neck cancers, with tumor heating to 43° C [14]. Lasers have been used in thermal ablation therapy for prostate cancer and retinoblastoma. High intensity focused ultrasound (HIFU) is also being exploited for tumor ablative heating of e.g., liver, prostate, and other cancers.

Numerous studies have demonstrated that hyperthermia enhances both chemotherapy (especially of alkylating agents) and radiotherapy [15]. In animal tumors, heating to 43.5° C for two hours with simultaneous X-ray irradiation gave a thermal enhancement ratio (ratio of

the radiation doses for radiation alone divided by radiation plus heat to produce the same therapeutic effect) of 8:1, making hyperthermia one of the most effective radiosensitizers known [3]. Hyperthermia also potentiates immunotherapy [16].

A major problem preventing the clinical implementation of hyperthermia has been the difficulty of heating tumors -- especially deep tumors -- more than the surrounding tissues. Further, there is also a time constraint in combining hyperthermia with radiation: the combination of hyperthermia and radiotherapy works best if the two are applied simultaneously, or at least within 1–2 hours of each other [3].

Gold nanoparticles (AuNPs) absorb light and have been explored as a method of heating. Spherical solid gold nanoparticles absorb light in the visible spectrum; 40 nm AuNPs with a peak absorption at 530 nm have been irradiated with a 514 nm laser to kill cells in vitro [17]. However, spherical AuNPs absorb only ultraviolet (UV) and visible light, so are generally poor choices for tissue heating since the penetration of UV and visible light in tissues is limited. The optimal wavelength for best tissue penetration is ~800 nm (near infrared, NIR). Gold nanoshells (~110 nm silica core with ~10 nm gold coating) were found to absorb in this range and were used to treat subcutaneous tumors in mice with good results using an intravenous (iv) injection followed by 800 nm laser irradiation [18]. These are now in clinical trials under the aegis of Nanospectra Biosciences for superficial head and neck cancers. Gold nanorods were similarly found to absorb at ~800 nm and used in treating subcutaneous murine tumors [19]. Although the optimal wavelength for tissue penetration is ~800 nm, there is still severe tissue attenuation (absorption and scattering), thus limiting this approach to superficial or directly accessible tumors.

Since solid spherical AuNPs do not absorb significantly at 800 nm, another approach is to have tumor cells take them up and aggregate them in endosomes and lysosomes [20–22]. When AuNPs aggregate, their absorption spectrum red-shifts [23, 24], which can be into the NIR. The advantages of using small AuNPs (e.g., 1–20 nm), compared to nanoshells (~130 nm) and nanorods (~50 nm) might be: a) better penetration into tumors[22, 25–28], and b) lower background absorption in non tumor cells and blood that do not aggregate the AuNPs (i.e., the small AuNPs ideally only aggregate and become NIR absorptive in the tumor while background amounts in normal tissue are unaggregated and NIR transparent and do not contribute to heating compared to NPs that are preformed to absorb NIR wherever they are).

Another advantage of using AuNPs in tumors is that they highly absorb X-rays, an effect that concentrates radiation absorption in the tumor, thus effectively increasing the radiotherapy dose [29–35]. Depending on the X-ray energy spectrum and the concentration of AuNPs in the tumor, the effective dose in the tumor can be increased by a factor of two or more [29].

In this study we report the combination of small 15 nm AuNPs that are aggregated in tumors with heating by NIR and exposure to X-rays. A substantial synergy was found, resulting in a significant reduction in the X-ray dose necessary to obtain the same therapeutic results reached with X-rays alone.

Materials and Methods

Gold Nanoparticles

Bare 15 nm AuNPs were prepared by citrate reduction: To 12 L of water, 60 mL of 2% tetrachloroauric acid ($HAuCl_4$) were added and the solution boiled. 360 mL of 1% sodium citrate (w/v) were then added and the solution boiled for 30 min. After cooling, 6 mL of 4N K_2CO_3 were added, adjusting the pH to 8.5. 1.8 mL of 1% SH-PEG2k-OCH_3 (dissolved in water) and 3.6 mL of 1% lipoic acid (dissolved in ethanol) were combined in 15mL of water. The PEG/Lipoic acid mixture was added to the Au solution. After 1 hour, the AuNPs were purified and concentrated to 100 mg Au/mL using a Minimate TFF system (Pall, Inc., Port Washington, NY, USA) overnight, then transferred to a 15 mL 100K membrane filter (Millipore, Billerica, MA, USA) to purify and concentrate further. 500 mg Au in Au-lipoic acid/PEG particles was obtained; gold yield = 83%. Gold core size was measured by transmission electron microscopy (FEI BioTwin G2 Transmission Electron Microscope, Hillsboro, OR, USA) and solution hydrodynamic diameter measured by dynamic light scattering (Brookhaven Instruments Corp. 90 Plus, Holtsville, NY, USA).

Absorption shift of AuNPs in cells

A431 tumor cells were incubated with or without 2 OD_{520} 15nm AuNPs for 2 days, then washed with PBS. Buffer was removed and dishes were placed vertically in the horizontal beam of a Hewlett Packard 8452A diode array spectrometer. Spectra were collected from 6 separate confluent cell areas.

Mice and tumors

6–8 week old male athymic nude mice (Charles River, Kingston, NY, USA) were implanted with murine squamous cell carcinoma (SCCVII) cells (American Type Culture Collection, Manassas, VA, USA) subcutaneously in their right legs. 200,000 cells in 25 μL were mixed with 25μL of Matrigel (BD Biosciences, San Jose, CA, USA) and used for implantation in each mouse. The time between cell implantation and treatments was 11 days. Before treatment, mice were anesthetized with 140 mg/kg ketamine and 3 mg/kg xylazine in phosphate buffered saline given intraperitoneally in about 0.06 mL. Tumor volume was estimated as half of the small diameter squared times the large diameter[36]. This study was carried out in strict accordance with the recommendations in the Guide for the Care and Use of Laboratory Animals of the National Institutes of Health. The protocol was approved by the Institutional Animal Care and Use Committee (IACUC) of the AALAC-approved University of Connecticut Health Center (UCHC) Center for Laboratory Animal Care (Assurance Identification Number: A2882-17, Protocol 210-622), and the Brookhaven National Laboratory IACUC (Protocol 419). All treatments were performed under anesthesia, and all efforts made to minimize discomfort and suffering.

MicroCT

Subcutaneous tumors on mice were imaged by microCT (Scanco VivaCT40, Bruttisellen, Switzerland). The source spot size was 5 μm at 45 kVp (with 0.5 mm Al filtering), sampling with 15×15×15 μm voxels.

Gold injections

A needle was placed in the center of the tumor mass and AuNPs delivered by Convection Enhanced Delivery (CED)[37] through PE-20 tubing connected to a syringe pump (Thermo Orion M361, Thermo Fisher Scientific, Waltham, MA, USA). The rate of injection was 4 μL/min and 100 μL of 100 mg Au/ml AuNPs were delivered to each tumor. Heating and irradiation were implemented 24 h later.

Biodistributions

Mice were infused by CED as described above with the treatment dose of either lipoic acid AuNPs or PEG AuNPs. 24 hours later, mice were dissected and tissues dissolved in aqua regia and Triton X-100, diluted in 0.5% HCl and analyzed for gold concentration by Inductively Coupled Plasma Mass Spectrometry (ICPMS, Agilent 7700× with helium collision cell, Santa Clara, CA, USA). Standards and QC checks were prepared from independent high purity standards (Spex-Certiprep, Metuchen, NJ and VHG Labs, Inc., Manchester, NH, USA).

Hyperthermia

Heat was applied using a water-filtered infrared A lamp (wIRA, Hydrosun model 750, Hydrosun Medizintechnik GmbH, Müllheim, Germany) with a 750 watt halogen lamp and a 780 nm high pass filter, yielding a peak output at 820 nm. This device is used in Europe to promote wound healing, treat warts, and other applications [38]. Although monochromatic lasers can also be used to provide NIR, the Hydrosun is simpler to operate, less expensive, safer, and has fewer regulatory restrictions. The dose rate is more than adequate to provide the necessary heating.

Tumors were irradiated at 1.5 W/cm^2. A circular mask 2.3 cm in diameter was placed over the leg to confine the radiation to the tumor region. The average tumor volume was 115 ± 69 mm^3 with an average diameter of ~5 mm, well within the 23 mm diameter heating circle. A 30 gauge thermocouple was placed in the tumor center. The lamp's intensity was controlled by a Variac, which was adjusted to cause the tumor to reach 48° C in 40 seconds, at which temperature it was then maintained for 5 minutes thereafter. An additional thermocouple was implanted subcutaneously in surrounding normal tissue 3 mm from the edge of the tumor that was in the heat-irradiated area to monitor its temperature. The average time between the end of heating and start of X-ray irradiation was 3 min, 9 sec ± 32 sec.

X-ray irradiation

Within minutes after heating, mice were irradiated with X-rays using a Philips RT100 X-ray generator (Philips International B.V., Amsterdam, The Netherlands) operating at 100 kVp with a 1.7 mm Al filter. The dose rate was 7.5 Gy/min at the tumor center, which was calibrated using a Radcal ion chamber (Monrovia, CA, USA). A collimator confined the region of irradiation to a 2.5 cm-diameter disk centered on the tumor. All doses were delivered in single fractions.

Results

The strategy employed in this study was to explore the synergy between hyperthermia and radiotherapy with the heating being provided by gold nanoparticles that absorb near infrared light. Although gold nanoshells and nanorods have been used for NIR heating, another approach used here is to employ much smaller solid gold nanoparticles (solid gold nanospheres). These, being smaller size, are likely to have better tumor penetration and the interesting property of only becoming NIR-absorbing after aggregation (Figure 1A). The AuNPs were constructed with a PEG and carboxylic acid shell with the two components adjusted such that the particles did not aggregate at pH 7.4, but were aggregated at lower pHs (Figure 1B).

The tumor environment is known to be acidic (pH <6.5) due to its high rate of metabolism and insufficient blood supply, resulting in buildup of lactic acid [39]. If the particles are taken up by the tumor cells, the endosomal pH is ~5.5, and when joined with the lysosome, the pH is 4–5 [40]. When incubated with cells, many of the AuNPs were internalized into endosomes and lysosomes (Figure 2A) and aggregated. At higher magnification, by electron microscopy, aggregation in the cells was apparent (Figure 2B). The spectra of cells incubated with AuNPs, then washed, showed considerable absorption in the NIR region, whereas cells without AuNPs hardly absorbed in this region (Figure 2C).

For in vivo testing, the nanoparticles can be injected either iv or directly into the tumor. Here we used direct intratumoral injection. Only a limited amount can be delivered intratumorally by rapid injection, and so we used concentrated AuNPs infused slowly at a rate of 4 μL/min, termed ‘convection-enhanced delivery’ (CED [37]). It provides a mild positive pressure, enough to essentially displace interstitial fluid. One conceptual problem with direct injection, although we found it effective in our approach, is that the AuNPs do not uniformly fill the tumor and do not completely avoid non-tumor tissue. X-ray images after a CED intratumoral injection of 15 nm PEG coated particles are shown in Figure 3. It can be noticed that a bolus remains at the injection site, but that some particles disperse in non-uniform directions and are shunted according to wherever the path has less resistance. Also, some of the particles appear to go into the leaky vasculature and then travel in blood vessels. Our infusion was continued until the injectate reached the tumor periphery (Figure 4A–C).

When these small AuNPs are directly infused intratumorally, the low pH of the tumor and the subsequent cell uptake we demonstrated resulted in their aggregation which rendered them capable of absorbing in the NIR. For direct intratumoral injection or infusion it is most desirable for the nanoparticles to spread throughout the tumor uniformly and if possible not go beyond the tumor edge. Practically, this is a difficult goal to obtain. We found that 15 nm PEGylated AuNPs spread too rapidly and after 24 hours could be seen a considerable distance from the tumor (Figure 4D). Also the coloration was red-purple (Figure 4D) comparable to the red color of the non-aggregated AuNPs (Figure 4E), indicating minimal aggregation. However, the lipoic acid AuNPs, which aggregate at tumor pH, were better confined to the tumor (Figure 4C) and also became black, indicating extensive aggregation of the AuNPs (Figure 4C). A biodistribution study quantified the levels of gold 24 hours

after infusion of the lipoic acid AuNPs vs. the PEG-only AuNPs (Supplemental Figure 1). The lipoic acid AuNPs had an average of 4.3 times more gold in the tumor compared to the PEG AuNPs which more extensively escaped the tumor and had considerably higher uptake in most other tissues.

The infused tumors were found to heat specifically and rapidly when exposed to NIR due to the absorption of aggregated AuNPs. This heating was combined with radiotherapy to study the synergy and therapeutic benefit that could be obtained. The experimental plan was to intratumorally infuse via CED the lipoic AuNPs, wait 24 hours for diffusion and cellular uptake, then heat with NIR at 48° C for 5 min, and within minutes irradiate with X-rays at various doses. Controls groups were ± AuNPs ± NIR ± X-rays. The experimental groups are detailed in Table 1.

The heating profiles are given in Figure 5. Results are given in Table 1 and Figure 6. The clear picture that emerges is:

1. Heating alone (48° C, 5 min, group B) is not effective at tumor control (1/7=14% survival, meaning 1 of 7 survived >250 days, and any survivors had no visible tumor).
2. 25 Gy alone or 25 Gy + NIR alone (without AuNPs NIR does not heat the tumor) is also not effective at tumor control (group A, radiation only, 2/6=33%, and group C, NIR + 25Gy, 0/7=0%).
3. AuNPs + 25Gy (group D) was also ineffective at tumor control (1/8=12%).
4. AuNPs + NIR heating + radiation was very effective. For the doses used, 15Gy, group E; 20Gy, group F; and 25Gy, group G, the resulting tumor control and survival values were 5/7=71%, 5/7=71%, and 5/7=71% respectively.
5. Controls of AuNPs-only or NIR-only showed no benefit (0/7=0% survival, Table 1).

Heating alone with AuNPs (group B) did not significantly slow tumor growth. As expected, all animals receiving radiation had delayed tumor growth for all tumors that progressed.

At the end of the experiment (day 250), the thigh thicknesses of the surviving animals were measured at the position of the original tumor and compared with the comparable thickness of the contralateral, untreated leg. Results are given in Table 2.

Although loss of muscle mass is evident in all survivors, there was no visually apparent loss in leg function and locomotion for any animal. It should also be noted that the average tumor diameter (4.9 mm) was the same as the normal leg diameter (4.9 mm), and an average loss of −21% corresponds to 1.0 mm, from which we surmise that the treatment was effective for a tumor with a margin projecting 1 mm deep into normal tissue - an ablation comparable to that achievable by careful surgical dissection.

Discussion

Heat has long been known to enhance radiotherapy, and hyperthermia has been termed one of the most effective radiosensitizers known [3]. However, it is not generally implemented clinically due to the difficulty of heating tumors specifically and the requirement that the heating and radiotherapy be done within about 1 hour of each other [3]. Our results here not only confirm this dramatic radiosensitization effect by heat, but also provide a way to specifically heat tumors and make it possible to combine the two in less than one hour. The strategy is to deliver AuNPs specifically to a tumor, apply NIR light that will predominantly heat only the tumor, and then deliver radiotherapy.

The results are surprising since the TCD50 (radiation dose needed to control 50% of the tumors) for extraordinarily radioresistant SCCVII tumors is 55.4 Gy [42]. Here we show that the TCD50 dose is < 15 Gy, yielding an effective treatment dose reduction factor of > 3.7. This should be highly beneficial clinically.

When no heating is involved, AuNPs in tumors are known to enhance radiotherapy by absorbing more of the incident X-rays, effectively increasing the dose deposited in the tumor. In this study, 100 mg Au/ml (10% by weight) was gently but steadily pressure-pumped into a tumor through one thin needle. If evenly distributed it would give a gold concentration of ~5% by weight, since tumor interstitial volume is ~50% [43]. This would be expected to give an X-ray dose enhancement factor of ~8 for the X-ray energy spectrum we used [29]. At a dose of 25 Gy, this should have certainly decimated the tumor. However, there were only 1 of 8 survivors, indicating poor response (Group D, Table 1). Also, this result was not better than 25 Gy alone (Figure 6A, D). Some gold may have escaped the tumor, but the most likely explanation is that the gold does not spread uniformly in the tumor (Figure 3), leaving much of it unenhanced. This underscores the severe limitation of treating tumors by direct intratumoral injections, an approach followed by many investigators. To realize a significant benefit, iv delivery appears to provide a much better tumor distribution [44, 45]. Intravenous delivery of AuNPs resulted not in homogeneous tumor distribution, but in virtually complete growing edge coverage [44]. Our data support the hypothesis that if the growing edge is completely destroyed, radioresistant internal cells can no longer survive. Radiotherapy combined with iv-administered AuNPs was therefore found to be effective at controlling tumors [30, 32, 45]. In this comparative study, direct infusion of the AuNPs yielded very high levels of gold irregularly dispersed within the tumor. Whereas it can be assumed that there was higher cell kill due to radiation enhancement in those regions, the inhomogeneity of this positive effect was not enough to be reflected in the median times for the tumors to reach 500 mm^3 (53 days for group A, 48 days for group C and 50 days for group D) or long-term survival. This failure additionally argues against therapies depending on full tumor coverage by direct injections. Further, it points out a significant difference between heating AuNPs vs. X-ray irradiating them. When AuNPs are heated by NIR, the heat spreads to surrounding cells that have small amounts of AuNPs or no AuNPs by conduction, convection, and radiative transfer, including blood flow. Therefore, an irregular gold distribution (Figure 3) may result in expanded regions of tumor being heated beyond the gold distribution. In the case at hand, mild hyperthermia by itself, 48° C for 5 min, is basically not therapeutic (Figure 6B), but is effective when combined with radiation (Figure

6E,F,G). In contrast, gold irradiated with X-rays does not produce heat and few ejected photoelectrons travel further than 100 μm[46], or about 10 cells. Therefore, closely spaced cells need to be adequately loaded with AuNPs, or such loading must encapsulate islands that can be cut off from their oxygen and nutrient supply, such as by surrounding the tumor, which can be achieved by iv delivery.[44] However, direct intratumoral loading of AuNPs is efficacious for hyperthermia when combined with radiotherapy. It retains the benefits of this mode of administration: a) high amounts can be given, which might be difficult to deliver by iv injection, b) low systemic toxicity, since most of the material remains localized, c) less concern about systemic clearance, and d) elimination of skin coloration sometimes encountered with iv injection of colored nanoparticles.

In the AuNPs + NIR heating groups, the precise temperature of the tumor cells at the exact tumor edge was not known. However, when combined with X-rays, results were efficacious. This implies that the heat either spread to reach these cells, increasing their radiosensitivity, or that cells at the growing edge of a tumor, which are known to be rapidly dividing and well oxygenated, are thereby more radiosensitive.

An additional design advantage of the method described here is the use of small AuNPs (here, 15 nm). Although efficient NIR-absorbing larger AuNPs have been studied (~130 nm gold nanoshells and 50 nm gold nanorods), there are two important advantages of using small AuNPs: 1) Diffusion and penetration into tumors will be better[22, 25–28]. 2) Tumor to non-tumor-background ratio is better with small AuNPs since small AuNPs, as individual particles, do not absorb in the NIR unless aggregated. Aggregation can be induced by the lower pH of the tumor milieu and endosomes/lysosomes or other mechanisms, such as by labile ligand bonds and lysosomal enzymes. Tumor uptake can be additionally made more specific by cell receptor targeting with antibodies, peptides or other moieties. Aggregation then only occurs in the tumor. This effect can contribute a powerful factor of tumor specificity since the particles will not absorb NIR if they are in surrounding normal tissues or blood. This was demonstrated in the current study where the 15 nm pH-sensitive particles that were designed to aggregate changed from red to black in the tumor (Figure 4C,E), while 15 nm particles that were not designed to aggregate showed little color change (Figure 4D). Additional evidence was seen in our heating data where tumors receiving aggregating AuNPs heated to 48°C upon exposure to NIR, but adjacent normal tissue under the same NIR only heated to 37°C, similar to the minor heating detected without AuNPs (Figure 5).

From our results, it was clear that the heating alone was very ineffective at tumor control (Figure 6B). This is consistent with findings from other studies noting that mild hyperthermia by itself is essentially ineffective [8, 30].

In this study 100 kVp X-rays were used at 7.5 Gy/min due to an available X-ray generator. Gold enhancement of X-rays is due to the photo- and Auger electrons produced and was found to be optimal at ~60 kVp.[47] However, substantial enhancement factors occur at higher and lower X-ray energies in the kilovolt range.[29, 32] Higher photon energies (up to 400 kVp) are needed clinically for penetration into deeper tissues.[34]

A limiting restriction of any NIR approach to heating is that at 800 nm the incident intensity is reduced to 10% after passing through 2.0 cm in tissue [48, 49]. Fiberoptic light pipes or laparoscopic techniques could be used to reach deeper tumors. Another limitation is that intratumoral injection is impractical for most human tumors. However, the effect should be significant for eligible cases. We have shown that direct injection of these small gold nanoparticles need not produce homogeneous gold distributions to be effective.

What is the prospect of gold nanoparticle hyperthermia approaches for clinical use? The approach described here appears to have the following advantages: 1) Combination of hyperthermia and radiotherapy can lead to a substantial, several-fold higher effectiveness of radiotherapy alone, 2) It provides a way to substantially reduce the radiotherapy dose and make it more tumor specific, 3) Initially smaller AuNPs may diffuse and penetrate tumors better than larger particles, 4) The tumor-specific low pH conversion of non-NIR-absorbing particles into absorbing ones through aggregation only in the tumor will give better tumor-to-non-tumor ratios, 5) Direct infusion allows adequate tumor loading that may be difficult to obtain by iv injections, 6) Direct infusion can drastically reduce systemic toxicity limits, 7) Direct infusion can reduce long term clearance issues compared to iv injection where most of the injected particles accumulate in the liver, spleen and other tissues with long-term retention and unknown long-term potential toxic effects, 8) A simple heating source can be readily available to all hospitals or even doctors' offices and third-world areas. NIR application is approved by the US FDA. Due to the limited penetration of NIR, certain superficial or accessible tumors (e.g. a subset of head and neck, and melanoma) would be immediate candidates, and the method could significantly improve clinical outcomes for those cancers.

In this report we show that small, 15 nm AuNPs have been designed to aggregate within tumors, and remain largely in the tumor, after direct intratumoral infusion, thus changing from NIR-transparent to NIR-absorbent, enabling tumor-specific heating upon NIR illumination. Heating of tumors to 48°C was easily achieved using a simple water-filtered halogen lamp NIR source, and, when combined with radiotherapy, was able to reduce the X-ray dose needed for tumor control by a factor >3, using only 15 Gy, yet leading to long-term (>250 days), tumor-free survival of most mice bearing an otherwise radioresistant lethal cancer.

Supplementary Material

Refer to Web version on PubMed Central for supplementary material.

Acknowledgments

The authors thank Mr. Daniel Sasso, Ms. Peggy Micca, Ms. Luping Qian, and Dr. John Dubendorff for technical assistance. This study was also supported by NIH grant 1R44CA130225 and the Dr. med. h.c. Erwin Braun Foundation.

References

1. Choi HS, Liu W, Misra P, Tanaka E, Zimmer JP, Itty Ipe B, et al. Renal clearance of quantum dots. Nat Biotechnol. 2007; 25:1165–70. [PubMed: 17891134]

2. Pandita TK, Pandita S, Bhaumik SR. Molecular parameters of hyperthermia for radiosensitization. Critical reviews in eukaryotic gene expression. 2009; 19:235–51. [PubMed: 19883367]

3. Horsman MR, Overgaard J. Hyperthermia: a potent enhancer of radiotherapy. Clin Oncol (R Coll Radiol). 2007; 19:418–26. [PubMed: 17493790]

4. Hinkelbein, W.; Bruggmoser, G.; Engelhardt, R.; Wannemacher, M. Preclinical Hyperthermia. New York: Springer-Verlag; 1988.

5. Sun X, Xing L, Ling CC, Li GC. The effect of mild temperature hyperthermia on tumour hypoxia and blood perfusion: relevance for radiotherapy, vascular targeting and imaging. Int J Hyperthermia. 2010; 26:224–31. [PubMed: 20230250]

6. Hildebrandt B, Wust P, Ahlers O, Dieing A, Sreenivasa G, Kerner T, et al. The cellular and molecular basis of hyperthermia. Crit Rev Oncol Hematol. 2002; 43:33–56. [PubMed: 12098606]

7. Nah BS, Choi IB, Oh WY, Osborn JL, Song CW. Vascular thermal adaptation in tumors and normal tissue in rats. Int J Radiat Oncol Biol Phys. 1996; 35:95–101. [PubMed: 8641932]

8. Lindner LH, Issels RD. Hyperthermia in soft tissue sarcoma. Current treatment options in oncology. 2011; 12:12–20. [PubMed: 21360087]

9. Jones E, Thrall D, Dewhirst MW, Vujaskovic Z. Prospective thermal dosimetry: the key to hyperthermia's future. Int J Hyperthermia. 2006; 22:247–53. [PubMed: 16754346]

10. Ruegg M, Moor U, Blanc B. A calorimetric study of the thermal denaturation of whey proteins in simulated milk ultrafiltrate. The Journal of dairy research. 1977; 44:509–20.

11. Uversky, VN.; Permyakov, EA. Methods in protein structure and stability analysis. New York: Nova Biomedical Books; 2007.

12. Simon CJ, Dupuy DE, Mayo-Smith WW. Microwave ablation: principles and applications. Radiographics : a review publication of the Radiological Society of North America, Inc. 2005; 25 (Suppl 1):S69–83.

13. Zheng Y, Li JQ, Chen MS, Zhang YJ, Zhang YQ. Comparison of shaft temperature related treatment efficacy between "air-cooled" microwave coagulation and traditional microwave coagulation. Chinese journal of cancer. 2004; 23:1477–81. [PubMed: 15566662]

14. Paulides MM, Bakker JF, Linthorst M, van der Zee J, Rijnen Z, Neufeld E, et al. The clinical feasibility of deep hyperthermia treatment in the head and neck: new challenges for positioning and temperature measurement. Phys Med Biol. 2010; 55:2465–80. [PubMed: 20371911]

15. Kampinga HH. Cell biological effects of hyperthermia alone or combined with radiation or drugs: a short introduction to newcomers in the field. Int J Hyperthermia. 2006; 22:191–6. [PubMed: 16754338]

16. Baronzio G, Gramaglia A, Fiorentini G. Hyperthermia and immunity. A brief overview. In Vivo. 2006; 20:689–95. [PubMed: 17203747]

17. El-Sayed IH, Huang X, El-Sayed MA. Selective laser photo-thermal therapy of epithelial carcinoma using anti-EGFR antibody conjugated gold nanoparticles. Cancer Lett. 2006; 239:129–35. [PubMed: 16198049]

18. O'Neal DP, Hirsch LR, Halas NJ, Payne JD, West JL. Photo-thermal tumor ablation in mice using near infrared-absorbing nanoparticles. Cancer Lett. 2004; 209:171–6. [PubMed: 15159019]

19. von Maltzahn G, Park JH, Agrawal A, Bandaru NK, Das SK, Sailor MJ, et al. Computationally guided photothermal tumor therapy using long-circulating gold nanorod antennas. Cancer Res. 2009; 69:3892–900. [PubMed: 19366797]

20. Nam J, Won N, Jin H, Chung H, Kim S. pH-Induced aggregation of gold nanoparticles for photothermal cancer therapy. Journal of the American Chemical Society. 2009; 131:13639–45. [PubMed: 19772360]

21. Hainfeld, JF. Methods and compositions for increasing infrared absorptivity of a target. US Patent Application 20080279946. 2008.

22. Hainfeld JF, O'Connor MJ, Lin P, Qian L, Slatkin DN, Smilowitz HM. Infrared-transparent gold nanoparticles converted by tumors to infrared absorbers cure tumors in mice by photothermal therapy. PloS one. 2014; 9:e88414. [PubMed: 24520385]

23. Khlebtsov B, Zharov V, Melnikov A, Tuchin V, Khlebtsov N. Optical amplification of photothermal therapy with gold nanoparticles and nanoclusters. Nanotechnology. 2006; 17:5167–79.

24. Su KH, Wei QH, Zhang X, Mock JJ, Smith DR, Schultz S. Interparticle coupling effects on plasmon resonances of nanogold particles. Nano Letters. 2003; 3:1087–90.
25. Kong G, Braun RD, Dewhirst MW. Hyperthermia enables tumor-specific nanoparticle delivery: effect of particle size. Cancer Res. 2000; 60:4440–5. [PubMed: 10969790]
26. Portet D, Denizot B, Rump E, Lejeune JJ, Jallet P. Nonpolymeric Coatings of Iron Oxide Colloids for Biological Use as Magnetic Resonance Imaging Contrast Agents. Journal of colloid and interface science. 2001; 238:37–42. [PubMed: 11350133]
27. Robinson JM, Takizawa T, Vandre DD. Enhanced labeling efficiency using ultrasmall immunogold probes: immunocytochemistry. The journal of histochemistry and cytochemistry : official journal of the Histochemistry Society. 2000; 48:487–92. [PubMed: 10727290]
28. Takizawa T, Robinson JM. Use of 1.4-nm immunogold particles for immunocytochemistry on ultra-thin cryosections. The journal of histochemistry and cytochemistry : official journal of the Histochemistry Society. 1994; 42:1615–23. [PubMed: 7983362]
29. Cho SH. Estimation of tumour dose enhancement due to gold nanoparticles during typical radiation treatments: a preliminary Monte Carlo study. Phys Med Biol. 2005; 50:N163–73. [PubMed: 16030374]
30. Hainfeld J, Dilmanian F, Zhong Z, Slatkin D, Smilowitz HM. Gold Nanoparticles Enhance Radiation Therapy of a Squamous Cell Carcinoma Growing in Mice. Phys Med Biol. 2010; 55:3045. [PubMed: 20463371]
31. Hainfeld JF, Dilmanian FA, Slatkin DN, Smilowitz HM. Radiotherapy enhancement with gold nanoparticles. J Pharm Pharmacol. 2008; 60:977–85. [PubMed: 18644191]
32. Hainfeld JF, Slatkin DN, Smilowitz HM. The use of gold nanoparticles to enhance radiotherapy in mice. Phys Med Biol. 2004; 49:N309–15. [PubMed: 15509078]
33. Kong T, Zeng J, Wang X, Yang X, Yang J, McQuarrie S, et al. Enhancement of radiation cytotoxicity in breast-cancer cells by localized attachment of gold nanoparticles. Small. 2008; 4:1537–43. [PubMed: 18712753]
34. McMahon SJ, Mendenhall MH, Jain S, Currell F. Radiotherapy in the presence of contrast agents: a general figure of merit and its application to gold nanoparticles. Phys Med Biol. 2008; 53:5635–51. [PubMed: 18812647]
35. Zhang SX, Gao J, Buchholz TA, Wang Z, Salehpour MR, Drezek RA, et al. Quantifying tumor-selective radiation dose enhancements using gold nanoparticles: a monte carlo simulation study. Biomed Microdevices. 2009; 11:925–33. [PubMed: 19381816]
36. Rofstad EK, Brustad T. Tumour growth delay following single dose irradiation of human melanoma xenografts. Correlations with tumour growth parameters, vascular structure and cellular radiosensitivity. British journal of cancer. 1985; 51:201–10. [PubMed: 3966977]
37. Bobo RH, Laske DW, Akbasak A, Morrison PF, Dedrick RL, Oldfield EH. Convection-enhanced delivery of macromolecules in the brain. Proc Natl Acad Sci U S A. 1994; 91:2076–80. [PubMed: 8134351]
38. Hartel M, Hoffmann G, Wente MN, Martignoni ME, Buchler MW, Friess H. Randomized clinical trial of the influence of local water-filtered infrared A irradiation on wound healing after abdominal surgery. The British journal of surgery. 2006; 93:952–60. [PubMed: 16845694]
39. Fukamachi T, Chiba Y, Wang X, Saito H, Tagawa M, Kobayashi H. Tumor specific low pH environments enhance the cytotoxicity of lovastatin and cantharidin. Cancer Lett. 2010; 297:182–9. [PubMed: 20831979]
40. Shen Y, Tang H, Zhan Y, Van Kirk EA, Murdoch WJ. Degradable poly(beta-amino ester) nanoparticles for cancer cytoplasmic drug delivery. Nanomedicine. 2009; 5:192–201. [PubMed: 19223244]
41. Remick DG, Xioa H. Hypothermia and sepsis. Frontiers in bioscience : a journal and virtual library. 2006; 11:1006–13. [PubMed: 16146792]
42. Yahiro T, Masui S, Kubota N, Yamada K, Kobayashi A, Kishii K. Effects of hypoxic cell radiosensitizer doranidazole (PR-350) on the radioresponse of murine and human tumor cells in vitro and in vivo. Journal of radiation research. 2005; 46:363–72. [PubMed: 16210793]
43. Jain RK. Transport of molecules in the tumor interstitium: a review. Cancer Res. 1987; 47:3039–51. [PubMed: 3555767]

44. Hainfeld JF, O'Connor MJ, Dilmanian FA, Slatkin DN, Adams DJ, Smilowitz HM. Micro-CT enables microlocalisation and quantification of Her2-targeted gold nanoparticles within tumour regions. Br J Radiol. 2011; 84:526–33. [PubMed: 21081567]

45. Hainfeld JF, Smilowitz HM, O'Connor MJ, Dilmanian FA, Slatkin DN. Gold nanoparticle imaging and radiotherapy of brain tumors in mice. Nanomedicine (Lond). 2012

46. Lechtman E, Chattopadhyay N, Cai Z, Mashouf S, Reilly R, Pignol JP. Implications on clinical scenario of gold nanoparticle radiosensitization in regards to photon energy, nanoparticle size, concentration and location. Phys Med Biol. 2011; 56:4631–47. [PubMed: 21734337]

47. Regulla DF, Hieber LB, Seidenbusch M. Physical and biological interface dose effects in tissue due to X-ray-induced release of secondary radiation from metallic gold surfaces. Radiat Res. 1998; 150:92–100. [PubMed: 9650606]

48. Bashkatov AN, Genina EA, Kochubey VI, Tuchin VV. Optical properties of human skin, subcutaneous and mucous tissues in the wavelength range from 400 to 2000 nm. Journal of Physics D-Applied Physics. 2005; 38:2543–55.

49. Ku G, Wang LV. Deeply penetrating photoacoustic tomography in biological tissues enhanced with an optical contrast agent. Optics letters. 2005; 30:507–9. [PubMed: 15789718]

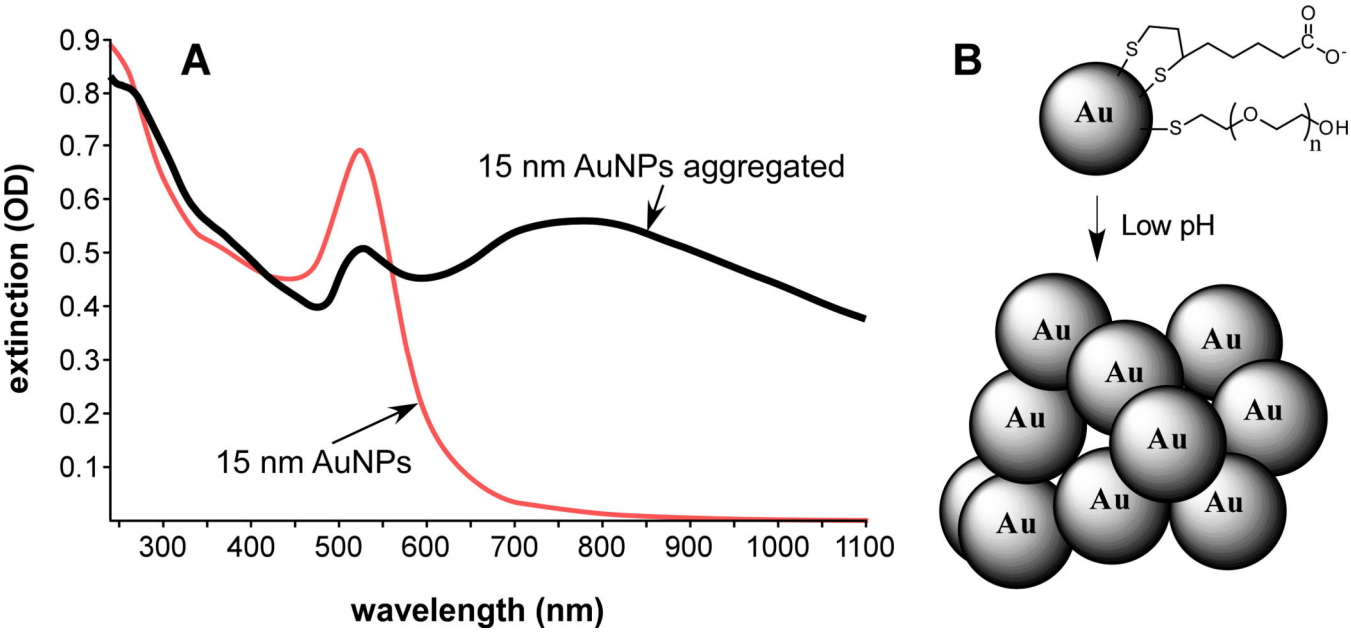

Figure 1.

(A) Change in spectra of 15 nm AuNPs before (red) and after (black) aggregation, here induced by lowering the pH to 5 in 150 mM NaCl. A large increase in the near infrared absorbance (750–1000 nm) is evident. **(B)** Aggregation of AuNPs at low pH. AuNPs coated with lipoic acid and PEG show aggregation at the pH of endosomes and lysosomes. Gold core size of the AuNPs was measured to be 15.3±1.0 nm by electron microscopy and the hydronamic diameter in solution was measured to be 21.6±0.1 by dynamic light scattering. The thiol ligands are not removed upon aggregation (here reversible with pH), but are not shown in the aggregated clump for clarity.

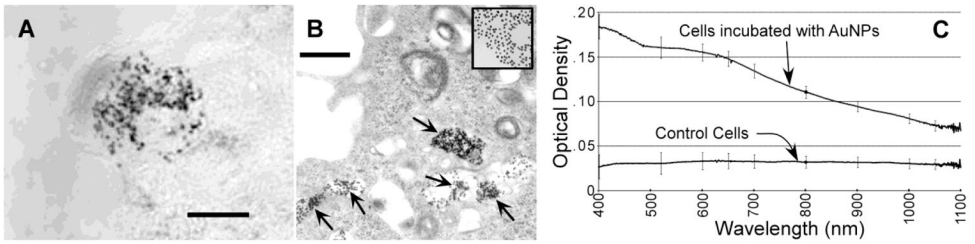

Figure 2.

(A) Light micrograph of the in vitro uptake and aggregation of lipoic acid AuNPs in the cytoplasm of one tumor cell. Bar = 10 μm. **(B)** Higher magnification electron micrograph of a cell after incubation with AuNPs. Aggregation of AuNPs can be seen in the endosomes/lysosomes. Inset at the same magnification shows unaggregated 15 nm AuNPs that exhibit the unaggregated spectrum shown in Figure 1A. Bar = 500 nm. **(C)** Spectra of cells incubated with or without AuNPs. Cells incubated with AuNPs showed absorption in the NIR region. Error bars are from 6 separate measurements.

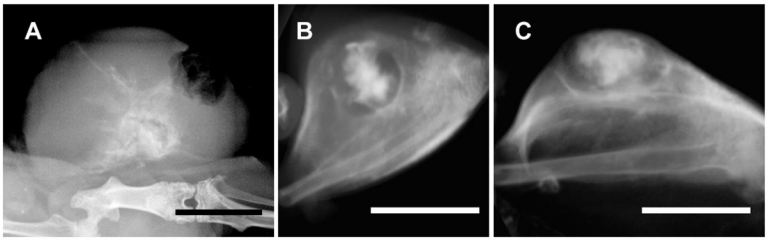

Figure 3.

X-ray images of tumors on mouse legs 24 hrs after a direct intratumoral injection by convection enhanced delivery (slow infusion over 25 min) of 15 nm AuNPs. **(A)** Planar X-ray image. **(B,C)** MicroCT images from top **(C)** and side **(D)** of another tumor. Bars = 0.5 cm.

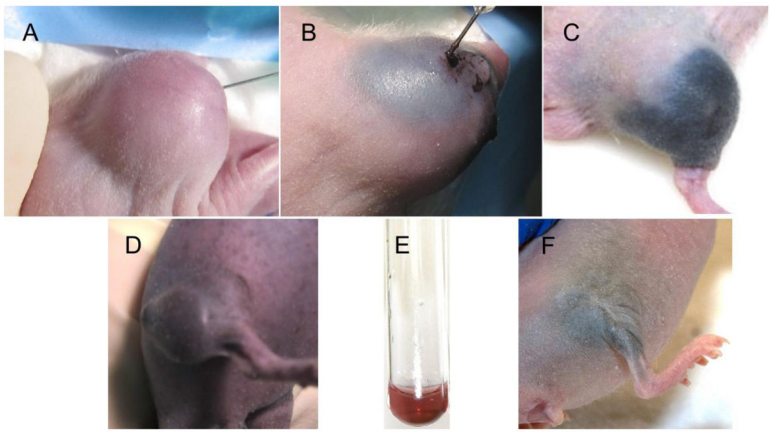

Figure 4.

Convection-enhanced delivery of AuNPs. **(A)**: Before injection; **(B)**: 20 minutes into injection; **(C)**: 24 hours after injection of lipoic acid AuNPs **(B,C)** which remain confined to the tumor region. **(D)**: 24 hours after injection of PEG-AuNPs which do not remain confined to the tumor region. **(E)**: Red color of 15 nm AuNPs. **(F)**: Treated mouse leg 250 days later.

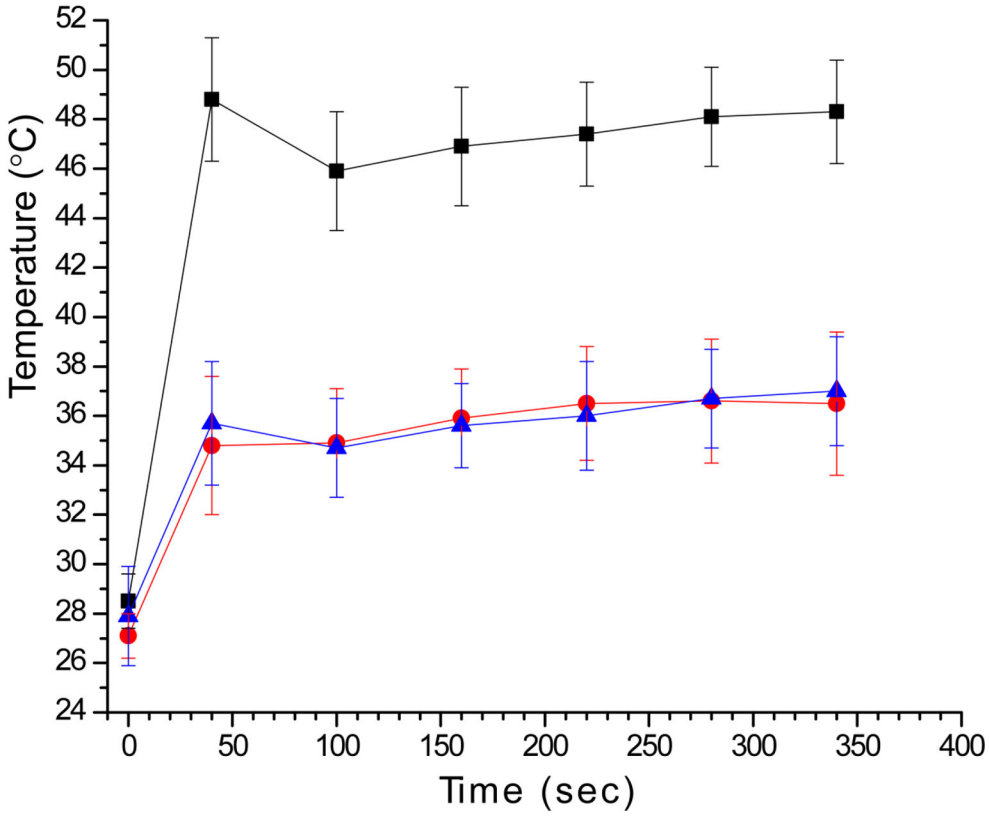

Figure 5.

Tumor and tissue heating profile. Black squares: tumor temperature during NIR exposure with AuNPs. Red circles: Subcutaneous temperature 3 mm away from tumor but in NIR field. Blue triangles: Tumor temperature during NIR exposure without AuNPs. Ketamine \xylazine anesthesia induces significant hypothermia explaining the low initial temperature.[41]

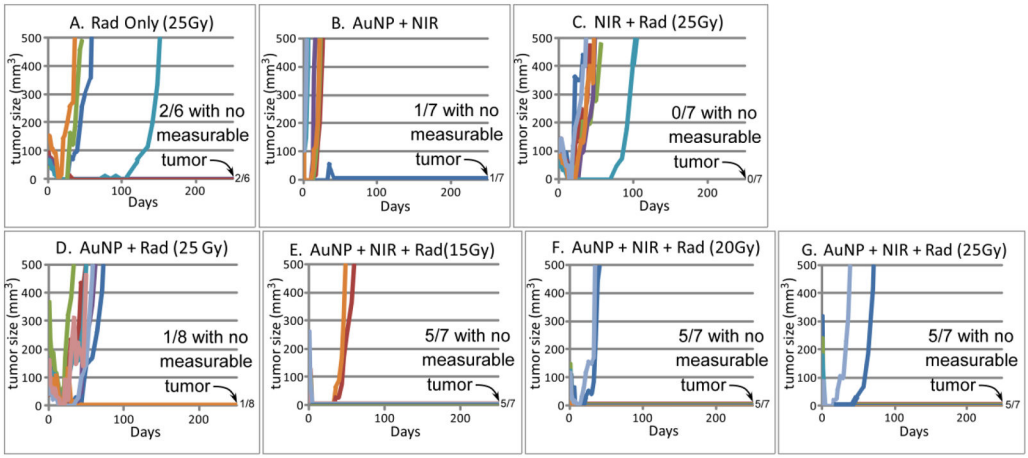

Figure 6.

Tumor volume vs. time for various treatments corresponding to Table 1. Survivors that were tumor-free at 250 days are given at the right of the horizontal axes (e.g., 5/7 meaning 5 out of 7 survived with no measurable tumor). Tumor volumes of individual mice are plotted. Each colored line represents one mouse.

Table 1

Experimental groups.

Group	AuNPs	NIR	Radiation 15 Gy	Radiation 20 Gy	Radiation 25 Gy	number of mice	survival (>250 days)
A					√	6	2/6=33%
B	√	√				7	1/7=14%
C		√			√	7	0/7=0%
D	√				√	8	1/8=12%
E	√	√	√			7	5/7=71%
F	√	√		√		7	5/7=71%
G	√	√			√	7	5/7=71%
H	√					7	0/7=0%
I		√				7	0/7=0%

Note: heating was only observed with AuNPs + NIR (Figure 5).

Nanomedicine. Author manuscript; available in PMC 2015 November 01.

Table 2

Average leg thickness change (%) compared to untreated contralateral leg for surviving animals (at 250 days).

Group	Average leg thickness change (%)
A	−21.7%
B	−37.2%
C	NA
D	−16.8%
E	−16.9%
F	−17.8%
G	−16.9%